*Carnegie Observatories Astrophysics Series, Vol. 1:
Coevolution of Black Holes and Galaxies, 2004
ed. L. C. Ho (Pasadena: Carnegie Observatories,
http://www.ociw.edu/ociw/symposia/series/symposium1/proceedings.html)*

Mass of the Central Black Hole and Gas Flow around it in Galaxies without and with Asymmetries

W. MACIEJEWSKI
Osservatorio Astrofisico di Arcetri, and Obserwatorium Astronomiczne Uniwersytetu Jagiellońskiego

Abstract

Various observables of gas dynamics in nuclear discs in galaxies are considered here. Long-slit spectrum of a gaseous disc around a central massive black hole may appear very complex even for thin discs in circular motion. The light distribution on the detector can be misinterpreted as coming from two distinct nuclear components. Fitting rotation curve to one component only discards about half of the light from the disc, and returns a faulty black hole mass. Original analysis of the STIS spectra of M84 may suffer from this omission. Asymmetries in galactic potentials induce dynamical resonances which perturb gas dynamics particularly in the central parts of galaxies. The perturbation often takes the form of a nuclear spiral, which can be described by the linear wave theory for weak spirals. For stronger ones, I present hydrodynamical models illustrating departures from this linear picture. The massive black hole in the galactic centre governs the resonances even beyond its classically defined sphere of influence, and therefore it should be able to regulate gas flow around itself.

1.1 Introduction

Gas in central parts of galaxies often exhibits well-organized behaviour: it settles in nuclear discs, which often host nuclear spirals (e.g. Verdoes Kleijn et al. 1999, Pogge & Martini 2002). Organized gas motions in galactic centres may yield information about Massive Black Holes (MBH) residing there (e.g. Macchetto et al. 1997). However, nearly-circular motions may be perturbed by asymmetries in galactic potentials that generate dynamical resonances. In §1.2, I explore a method that determines the MBH mass from gas kinematics in the nuclear disc observed through a long-slit. I focus on complex patterns in the observed spectrum that can give a misleading impression of the structure in the nuclear gas, but when interpreted correctly, they can have considerable diagnostic power. In §1.3, I define the dynamical resonances generated by asymmetries in the potential, and explain how the central MBH can move or erase them. I analyze the gas flow around the resonances, and in particular strong and weak nuclear spirals.

1.2 Long-slit Spectra of a Thin Axisymmetric Gaseous Disc

Effects described here may appear on the detector of a spectrograph that uses slit wider than the instrumental point-spread function. This practice is particularly common for the STIS spectrograph on the Hubble Space Telescope, where it enhances the signal-to-noise ratio (S/N) of the data at the price of what is thought to be merely an insignificant loss in

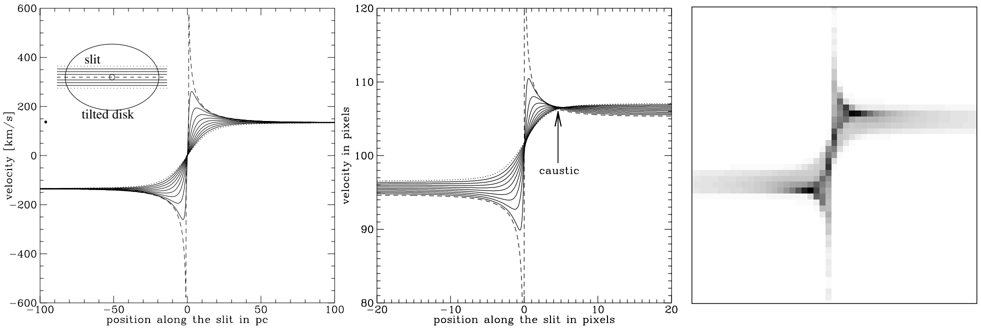

Fig. 1.1. *Left:* Position-velocity diagram for the disc inclined at 60°, rotating in a potential of a 10^8 $M_\odot$ BH plus extended density distribution $\sim R^{-1.8}$. Velocities are sampled along cuts parallel to the line of nodes, shown in the inset at upper left. *Centre:* The light-pattern on the spectrograph's detector (only half of the slit width is sampled) *Right:* The light from entire slit integrated within the detector's pixels.

velocity resolution. However, when the target has arbitrarily large velocity gradients, the use of a wide slit can have more subtle effects, and complex light-patterns appear on the detector. Details of this work can be found in Maciejewski & Binney (2001).

Consider a thin gaseous disc placed in an axisymmetric galactic potential including a MBH at its centre. If the disc is in circular motion, emission-line spectrum observed through a long-slit spectrograph with a slit placed along the line of nodes should tell us about rotation velocities of the gas. However, if the slit is wider than the instrumental point-spread function, then features *across* the slit can be resolved. Thus in addition to the rotation curve, which is Keplerian in the innermost part (dashed line in Fig.1.1, left), a wide slit samples off-centre velocities, which vanish at the galaxy centre (solid lines in Fig.1.1, left). The spectrograph further modifies light pattern on the detector, because features resolved across the slit translate on the detector into points separated in the dispersion direction. Thus both, position across the slit and the velocity information, appear entangled on the detector as shifts along the dispersion direction. To reflect the light pattern on the detector, the left panel of Fig.1.1 has to be modified by shifting each sample line in the dispersion direction by a constant amount, different for each line (central panel of Fig.1.1). As a result, at large radii, where rotation velocities are roughly constant, the observed spectrum is widened by the width of the slit. At small radii, the profile widens because rotation velocities vary across the slit. The Doppler shifts compete with the position offsets across the slit, and at some intermediate radius they are equal: light from all positions across the slit converges at one effective velocity, forming *the caustic*. At radii interior to the caustic, two maxima in the light distribution are present (Fig.1.1, right): one from the slit centre (showing Keplerian rise), and one from the slit edges (passing through zero velocity at the nucleus). Thus position-velocity diagrams for rotating discs are rich in structure; the information contained in it is lost if one merely fits a Gaussian emission line profile at each radius (which is the traditional approach).

The light-pattern predicted above has been actually observed in the most detailed long-slit spectrum of nuclear emission so far (M84, Bower et al., 1998), where two light-maxima

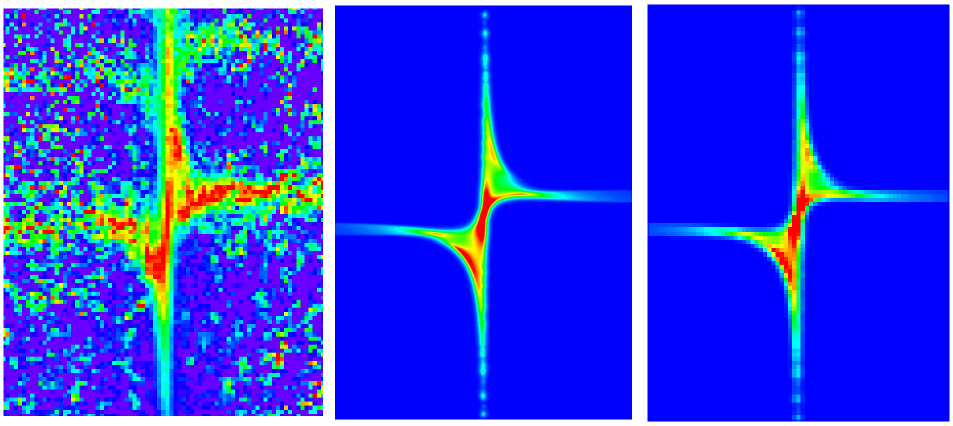

Fig. 1.2. *Left:* an $H\alpha$ emission-line spectrum of M84 taken with STIS using the G750M grating (from Bower et al. 1998). The dispersion direction is vertical. *Centre:* a modeled light distribution on the spectrograph's detector (convolved with instrumental PSF) for $i = 74°$, PA $= 21°$, $M_\bullet = 4 \times 10^8 M_\odot$, and the centre of the slit shifted by 0.03 arcsec from the nucleus. The distance to M84 has been taken to be 17 Mpc and the surface-brightness of the emission has been assumed to be proportional to $R^{-1.5}$. *Right:* light distribution from the central panel integrated over detector pixels.

are seen at radii close to the nucleus (Fig.1.2, left). In the original data analysis, these maxima were interpreted as coming from two physically distinct nuclear components, but the analysis above indicates that they are caused by a wide slit. Fitting rotation curve to only one component discards about half of the light from the disc, and returns a faulty MBH mass. On the other hand, the position of the caustic along the slit is quite independent of the stellar density profile, and it can indicate the presence, and betray the mass of the MBH (see Maciejewski & Binney 2001 for details). In principle, it gives enough information to recover the disc's inclination angle and the MBH mass independently. They turn out to be 74°, and 4×10^8 $M_\odot$. The mass of the MBH is smaller than the estimate of Bower et al. by a factor of 4. The reason for this discrepancy is that Bower et al. fitted only one component of the integral light-pattern on the detector, while *the whole pattern* of the nuclear spectrum of M84 can be explained as coming from a thin disc in circular motion (Fig.1.2, right), and the whole pattern must enter into the MBH mass determination. If this pattern is modeled with adequate sophistication, it can have considerable diagnostic power.

Surprisingly, M84 was excluded from the Tremaine et al. (2002) sample of galaxies used to determine the correlation between the MBH mass and the bulge properties. It was rejected because various MBH mass estimates there differ by a factor of four. On the other hand, the very reason for having various estimates is the excellent quality of the data, welcoming various analyses. If we exclude this data, we are bound to base the correlation on data of essentially inferior quality, for which only one MBH mass estimate has been done, obviously not controversial.

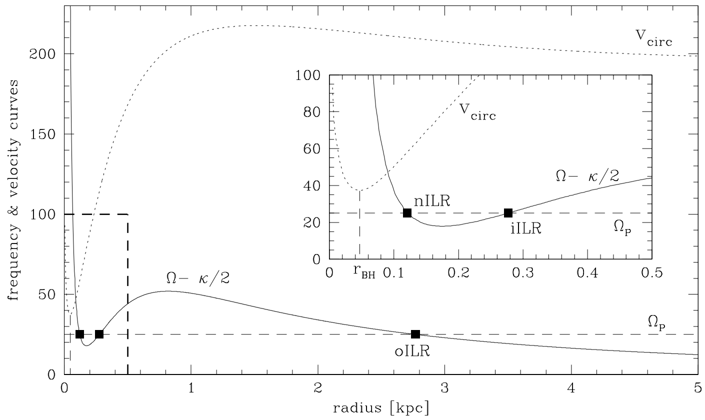

Fig. 1.3. Velocity and frequency curves for a potential with 3 ILRs. The circular velocity ($v_{\rm circ}$) is drawn with dotted line, the frequency curve is solid. The constant pattern speed Ω_P is marked with the horizontal dashed line. Positions of the three ILRs: nuclear (nILR), inner (iILR), and outer (oILR) are marked with squares. A close-up of the inner region is shown in the insert, where the sphere of influence of the $10^7 M_\odot$ MBH has roughly the radius $r_{\rm BH}$.

1.3 Gas Flow around the Central MBH in Asymmetric Potentials

Gas flow in the nuclear discs in galaxies may differ from simple circular motion. Even weak asymmetries in galactic potentials perturb gas dynamics, and generate waves in gas. The strongest perturbations occur around resonances, where a gas cloud is a subject to a monotonic force from the potential. In the nuclear region, Inner Lindblad Resonances (ILR) form when the mass is sufficiently centrally concentrated. They cause strongly non-circular motions and shocks in gas (Athanassoula 1992, Wada 1994). If a galaxy has a central MBH, it must have at least one ILR. The resonance caused directly by the MBH is called the nuclear ILR, and it is located at the radius a few times larger than the MBH's radius of influence (minimum of the rotation curve, Fig.1.3). A pair of shocks in gas flow may form at this resonance (Fukuda et al. 1998), which can be used in MBH mass estimates, while the conventional methods of stellar kinematics require information from smaller radii. On the other hand, shocks around the nuclear ILR strongly disturb gas kinematics; if they are present, the assumption of a circularly rotating disc, common when the MBH mass is derived from kinematics of ionized gas (e.g. Macchetto et al. 1997), may no longer be valid.

Alternatively, the ILR may be caused by the integrated central mass concentration in the galaxy, and not by the MBH only. Such an ILR occurs at larger radii (up to a few kpc), and it is called the outer ILR, but gas flow around it is similar to that around the nuclear ILR. Strong asymmetries in the potential may generate shocks that extend even outside the outer ILR (Athanassoula 1992). These shocks are almost straight at large radii, but they may wind up into a nuclear spiral well inside the outer ILR (Maciejewski et al. 2002). The wave nature of the nuclear spirals was well pointed out by Englmaier & Shlosman (2000). However, as I show below, these waves turn into shocks for strong asymmetries in the potential, and the linear description proposed by Englmaier & Shlosman is a rough approximation only. On

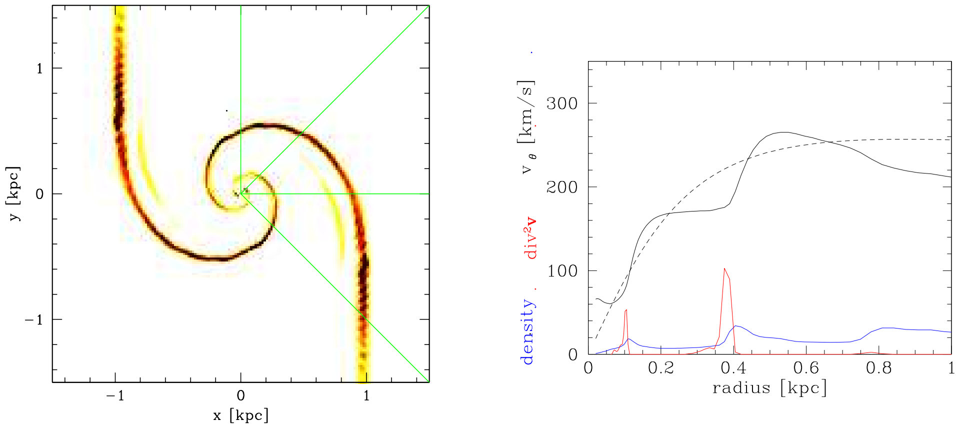

Fig. 1.4. Nuclear spiral in a strong bar. *Left:* The shape of the spiral, as traced by negative *div***v** in gas. *Right:* Tangential gas velocity (solid line) with circular rotation curve drawn for comparison with a dashed line. Red line marks negative *div***v**, and density profile is shown with a blue line. All lines drawn for a cut running from the galaxy centre into the bottom-right corner of the left panel.

the other hand, even very weak asymmetries in the potential trigger gaseous density waves *inside* the outer ILR (Maciejewski 2001) in a form of nuclear spirals.

I have built two hydrodynamical models of the nuclear spiral. One spiral forms in a potential with strong asymmetry, caused by a bar similar in strength to that of the standard model by Athanassoula (1992). The other one is generated in a potential with a weak oval asymmetry, whose quadruple moment is 10 times smaller than that of the bar in the previous model. In the first model (Fig.1.4), two straight shocks form across the outer ILR of the bar (which is located at 2.1 kpc), in accordance with our understanding of gas flow in a bar (Athanassoula 1992). Well inside the outer ILR, these shocks curl into a spiral, but they are still shocks, as is indicated by the large negative *div***v** (strongly convergent flow) in the spiral. I made a sample cut through the nuclear spiral that shows how would the velocity field look like when seen through a long slit. A plot in Fig.1.4 shows the extracted 'rotation curve'. Departures from circular rotation are very large, even in the innermost parts of the spiral. Although the spiral has a wave nature, it does not follow the linear theory: instead of winding up a number of times, it quickly opens in order to match the straight shock in the bar.

In the second model (Fig.1.5), the asymmetry in the potential is very weak, and there are no straight shocks similar to those caused by the bar in the first model. However, the weak oval distortion is strong enough to generate a tightly wound nuclear spiral. The density contrast between the arm and the inter-arm region is about 2, therefore the spiral should be clearly visible in the color maps. On the other hand, the perturbation of the velocity field is small: gas flow in discs with such tightly-wound spirals is almost circular, and methods

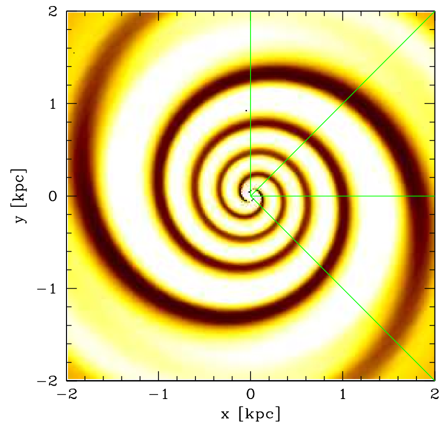

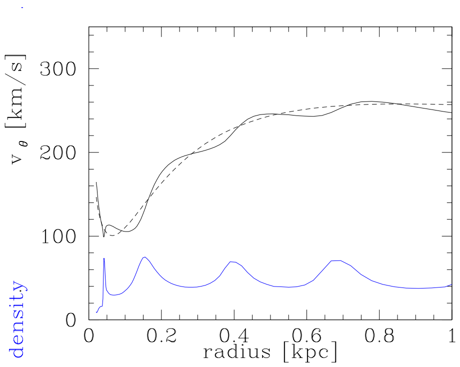

Fig. 1.5. Nuclear spiral in a potential of a weak oval. *Left:* The density distribution inside the ILR. *Right:* Tangential gas velocity, circular velocity and gas density marked as in Fig.1.4.

based on gas kinematics should yield a reliable MBH mass. Unlike the previous model, this spiral is a weak density wave, and it follows the linear theory, which keeps it tightly wound at increasing radii. Thus tightly-wound nuclear spirals are related to weak asymmetries in the potentials. The linear theory of non-selfgravitating gas predicts that the nuclear spiral should not extend beyond the outer ILR, and that if another ILR is present inside it, it should not propagate inwards of this ILR. Nuclear spirals extending all the way to the centres of galaxies indicate that only the outer ILR is present there.

1.4 Conclusions

Gas flow around the central MBH can have considerable diagnostic power, but to utilize this power one has to analyze gas kinematics very carefully. In particular, instrumental effects can alter the long-slit spectrum significantly, but the altered spectrum shows patterns (caustic, two light-maxima) that are useful in the MBH mass estimates. These patterns occur even for a thin disc in circular rotation.

Dynamics of the nuclear gas is much more complex in the presence of asymmetries in the galaxy potential. Shocks around the nuclear ILR, and spiral shocks well inside the outer ILR can alter gas kinematics to the extent that the standard gas-kinematical methods to measure the MBH mass cannot be applied anymore. Note however that shocks at the nuclear ILR can themselves serve as the MBH indicator. On the other hand, weak, tightly wound nuclear spirals have little kinematical effect, and they should not affect the MBH mass estimate. These spirals indicate also that there are no other ILRs in the zone of their presence, which gives us additional information about mass distribution in the galaxy centre.

References

Athanassoula, E. 1992, MNRAS, 259, 345

Bower, G. A., et al. 1998, ApJ, 492, L111
Englmaier, P. & Shlosman, I. 2000, ApJ, 528, 677
Fukuda, H., Wada, K., & Habe, A. 1998, MNRAS, 295, 463
Macchetto, F., Marconi, A., Axon, D. J., Capetti, A., Sparks, W., & Crane, P. 1997, ApJ, 489, 579
Maciejewski, W. 2001, in The Central Kpc of Starbursts and AGN: The La Palma Connection, ed. J. H. Knapen et al. (San Francisco: ASP), 153
Maciejewski, W., & Binney, J. 2001, MNRAS, 323, 831
Maciejewski, W., Teuben, P. J., Sparke, L. S., & Stone, J. M. 2002, MNRAS, 329, 502
Pogge, R. W., & Martini, P. 2002, ApJ, 569, 624
Tremaine, S., et al. 2002, ApJ, 574, 740
Verdoes Kleijn, G. A., Baum, S. A., de Zeeuw, P. T., & O'Dea, C. P. 1999, AJ, 118, 2592
Wada, K. 1994, PASJ, 46, 165